ELSEVIER

Journal of Alloys and Compounds 317–318 (2001) 227–232

Journal of ALLOYS AND COMPOUNDS

www.elsevier.com/locate/jallcom

Neutron diffraction study of magnetic ordering of two binary uranium tellurides U_3Te_5 and U_2Te_3

O. Tougait[a], G. André[b], F. Bourée[b], H. Noël[a,*]

[a]*Laboratoire de Chimie du Solide et Inorganique Moléculaire, UMR CNRS 6511, Université de Rennes 1, Avenue du Général Leclerc, 35042 Rennes, Cedex, France*

[b]*Laboratoire Léon Brillouin (CEA-CNRS), CEA/Saclay, 91191 Gif-sur-Yvette, France*

Abstract

The binary uranium tellurides U_3Te_5 and U_2Te_3 have been studied by neutron powder diffraction as a function of temperature. In the case of U_3Te_5 (*Pnma* space group), the magnetic moments of the three uranium sites (U_1, U_2, U_3) are lying in the *a*–*c* plane with a F_xC_z -type structure, with different magnetic moments for U_1, U_2, U_3. A spin reorientation towards the *c* direction occurs around $T=45$ K. Neutron diffraction data for U_2Te_3 (*Pnma* space group) are consistent with an antiferromagnetic G_x A_z -type structure. The magnetic moments of uranium atoms in two crystallographic sites (U_1, U_2) are in the *a*–*c* plane with different magnetic moments for U_1 and U_2. A slight spin reorientation on the U_2 site occurs around $T=45$ K. Close to the ordering temperature, hints of a complex magnetic structure can be detected. In both compounds, these results are correlated with the macroscopic magnetic measurements. © 2001 Elsevier Science B.V. All rights reserved.

Keywords: Uranium tellurides; Magnetic structures; Neutron diffraction

1. Introduction

The binary uranium tellurides U_3Te_5 and U_2Te_3 have been recently characterized by single crystal X-ray diffraction and bulk magnetic measurements [1,2]. U_3Te_5 crystallizes in the orthorhombic space group *Pnma* (no. 62) with four formula units in a cell of dimensions, $a=16.098(7)$ Å, $b=4.210(2)$ Å, $c=14.060(4)$ Å. The three non equivalent uranium atoms, lying on *4c* Wyckoff positions, are each surrounded by eight neighboring Te atoms in a bicapped trigonal prism environment. The three prisms are connected to each other by edge sharing to form a large hexacapped trigonal prism. The crystal structure of U_3Te_5 consists in a three-dimensional arrangement of these large triprisms. They share their triangular faces along the *b* axis and are joined by sharing two edges to form infinite zigzag chains, running in the *a*–*c* plane. These chains are shifted one to each other by $b/2$. Magnetic measurements (Fig. 1) reveal that U_3Te_5 orders ferromagnetically below $T_c=117$ K; the change of slope of the magnetization around 45 K, may be related to a spin reorientation.

U_2Te_3 crystallizes in the orthorhombic U_2S_3 structure type, (space group *Pnma*) with four formula units in a cell of dimensions $a=12.175(2)$ Å, $b=4.370(1)$ Å, $c=11.828(2)$ Å. Each uranium atom lies on a *4c* position and adopts a 7-fold coordination of tellurium atoms in two different motifs; the first (U_1) within a polyhedron related to an octahedron in which one apex is split into two positions, the second (U_2) in a monocapped trigonal prism environment. The polyhedra share either triangular faces, in the case of trigonal prisms, or edges, in the case of 7-octahedra with their neighboring units forming infinite columns along the *b* axis. In the *a*–*c* plane, the columns are connected by sharing common Te atoms and edges. In agreement with previous magnetic measurements [3], U_2Te_3 exhibits a complex magnetic behavior below 110 K (Fig. 2). The thermal variation of the magnetization shows a sharp maximum at $T=105$ K, followed by a local minimum at $T=96$ K. Upon cooling the sample, a subsequent discontinuity occurs around 45 K, may be associated with a spin reorientation.

In order to explain the unusual magnetic features of U_3Te_5 and U_2Te_3, a neutron powder diffraction study has

*Corresponding author.

E-mail address: henri.noel@univ-rennes1.fr (H. Noël).

0925-8388/01/$ – see front matter © 2001 Elsevier Science B.V. All rights reserved.
PII: S0925-8388(00)01333-5

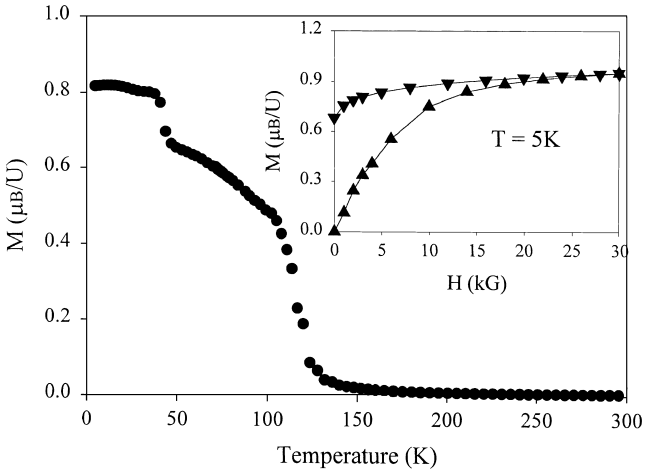

Fig. 1. Magnetization versus temperature and magnetic field for U_3Te_5.

been undertaken as a function of temperature. Here, we report for both compounds the magnetic structures obtained at low temperature and their thermal evolution.

2. Experimental

U_3Te_5 and U_2Te_3 were synthesized from the elements in stoichiometric proportions mixed with a small quantity of CsCl (1/10 in weight) [1,2] in a sealed quartz tube. The samples were gradually heated and held at 700°C for several days. The final products were rapidly washed with alcohol at 70% to remove the major part of the alkaline chloride salt and dried with acetone. Samples were then ground in an argon glove box to a grain size of about 100 μm. Neutron diffraction experiments were performed at the Laboratoire Léon Brillouin (C.E.A.-Saclay, France) on the G4.1 multidetector powder diffractometer. Each powder sample (6 g) was held in a vanadium container and inserted into a He cryostat. Data sets were collected in the temperature range $1.4 < T < 155$ K. The Rietveld refinements were performed using the program FULLPROF [4], and CsCl was introduced as a minor impurity phase in the refinement procedure.

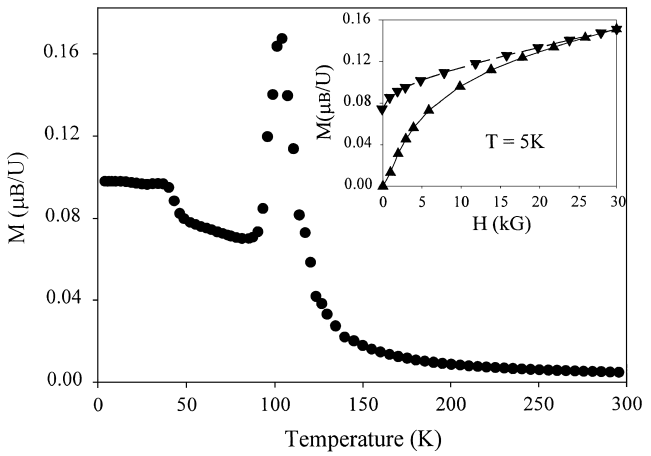

Fig. 2. Magnetization versus temperature and magnetic field for U_2Te_3.

Neutron diffraction patterns at temperatures above the respective ordering temperatures were refined using the single crystal X-ray results as initial models [1,2]. The refinements of the crystal structures converged rapidly and confirmed the purity of the samples, free of other uranium compound impurities.

3. Neutron diffraction results

3.1. U_3Te_5 crystal and magnetic structures

The neutron powder diffraction data analysis confirms the previous X-ray U_3Te_5 structure determination (see Table 1 for partial results on the refined parameters) and shows that no structural transition occurs in the temperature range 1.4–300 K.

Fig. 3 shows the neutron powder diffraction diagram for U_3Te_5 at $T = 1.4$ K: for this temperature both crystal and magnetic contributions have to be taken into account in the refinement. All magnetic Bragg peaks can be indexed within the chemical unit cell, i.e. with a propagation vector $k = (0\ 0\ 0)$. Fig. 4 shows the thermal variation of the integrated intensity of some characteristic peaks. From these thermal variations, the magnetic transition temperature is 115 ± 5 K, in good agreement with magnetic measurements. Another magnetic 'transition' is observed at $T = 45 \pm 5$ K.

Applying Bertaut's representation analysis of magnetic structures [5] to *Pnma* space-group, $k = (0\ 0\ 0)$ propagation vector and (*4c*) Wyckoff position leads to the subsequent magnetic space groups and magnetic structures:

Table 1
U_3Te_5: refined cell parameters and atomic coordinates for U atoms, from neutron powder diffraction data at $T = 131$ K and $T = 1.4$ K; reliability factors R_B and R_M are calculated for nuclear and magnetic contributions, respectively

		$T = 131$ K	$T = 1.4$ K
a (Å)		16.119(2)	16.113(2)
b (Å)		4.2128(5)	4.2013(5)
c (Å)		14.079(2)	14.076(2)
U_1	*x*	0.1292(6)	0.1278(7)
	z	0.4131(9)	0.4123(9)
U_2	*x*	0.3598(7)	0.3610(7)
	z	0.5657(9)	0.5671(9)
U_3	*x*	0.3815(7)	0.3773(9)
	z	0.2525(7)	0.2529(9)
R_B [a]		4.42	4.62
R_M [a]			8.28
No. of refined parameters		26	32

[a] Reliability factors are defined in Ref. [4].

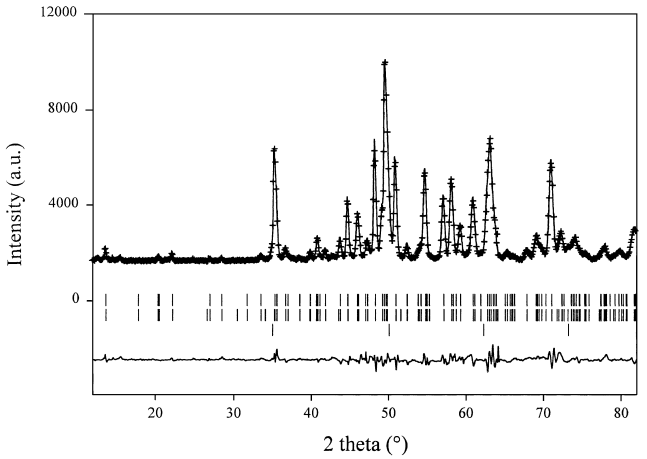

Fig. 3. U_3Te_5, $T=1.4$ K: experimental (dots) and calculated (solid line) neutron powder diffraction diagram; difference curve below. The ticks, respectively indicate the 2θ values for nuclear and magnetic Bragg peaks of U_3Te_5 (upper and middle row) and nuclear Bragg peaks of CsCl (lower row).

Pnma		C_y	
Pnm′a′	F_x		C_z
Pn′ma′		F_y	
Pn′m′a	C_x		F_z
Pn′m′a′	A_x		G_z
Pn′ma		G_y	
Pnm′a	G_x		A_z
Pnma′		A_y	

where F, G, C and A are associated with the respective sequences of magnetic moments: $F=S_1+S_2+S_3+S_4$ (ferromagnetic); $G=S_1-S_2+S_3-S_4$ (antiferromagnetic); $C=S_1+S_2-S_3-S_4$ (antiferromagnetic); $A=S_1-S_2-S_3+S_4$ (antiferromagnetic) and S_1, S_2, S_3 and S_4 stand for the four magnetic moments of atoms in a (*4c*) Wyckoff site, i.e. in x, 1/4, z, (1); $1-x$, 3/4, $1-z$, (2), $1/2-x$, 3/4, $1/2+z$, (3) and $1/2+x$, 1/4, $1/2-z$, (4).

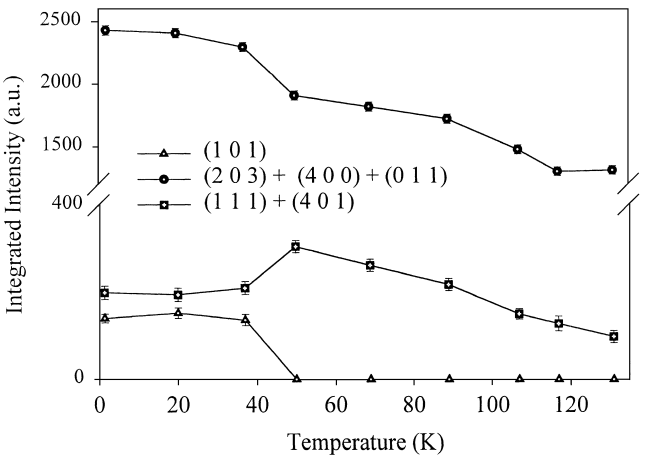

Fig. 4. U_3Te_5: thermal variation of the integrated intensity of some characteristic peaks.

Table 2
U_3Te_5: refined magnetic moments for U_1, U_2 and U_3, from neutron powder diffraction data at T ranging from 1.4 to 107 K; reliability factors R_B And R_M are calculated for nuclear and magnetic contributions, respectively

T (K)	R_N (%)	R_M (%)	M U_1 (μ_B)	M U_2 (μ_B)	M U_3 (μ_B)
1.4	4.62	8.28	1.84(10)	0.98(20)	1.83(10)
20	4.20	8.36	1.76(14)	0.78(24)	1.86(10)
37	4.27	9.65	1.99(10)	1.10(23)	1.44(10)
50	4.52	10.2	1.84(14)	0.90(20)	1.39(19)
69	4.56	10.7	1.72(14)	0.93(20)	1.40(15)
89	4.26	12.5	1.41(18)	0.77(18)	1.50(18)
107	4.88	15.7	0.90(20)	0.98(27)	0.76(15)

The best agreement with the low temperature neutron powder diffraction diagrams is obtained, whatever the temperature below 115 K, for the non-collinear F_x C_z type-structure. Table 2 lists the results of these magnetic refinements, in terms of magnetic moment values for U_1, U_2, U_3 and reliability factors. Below $T_C=115$ K, the magnetic order of the three independent uranium atoms (U_1, U_2, U_3) is non-collinear, with for each of the uranium sublattices, a ferro- and an antiferromagnetic component in the a–c plane. Along the a axis, the magnetic moment components are ferromagnetically coupled to each other, whereas along the c axis, the components exhibit a double antiparallel alignment between adjacent triprisms within the chain and triprisms of neighbouring chains.

Table 2 shows that each U magnetic moment has a different amplitude and Table 3 that the direction of the magnetic moments relative to the crystal axis a and c changes with T. At $T=1.4$ K, the U_1 and U_3 magnetic moments are almost aligned along the a axis, whereas the U_2 magnetic moment is almost parallel to the c axis (Fig. 5). At $T=50$ K (Fig. 5), U_1 and U_2 magnetic moments remain nearly unchanged, whereas U_3 magnetic moments are rotated towards the c axis. This reorientation process,

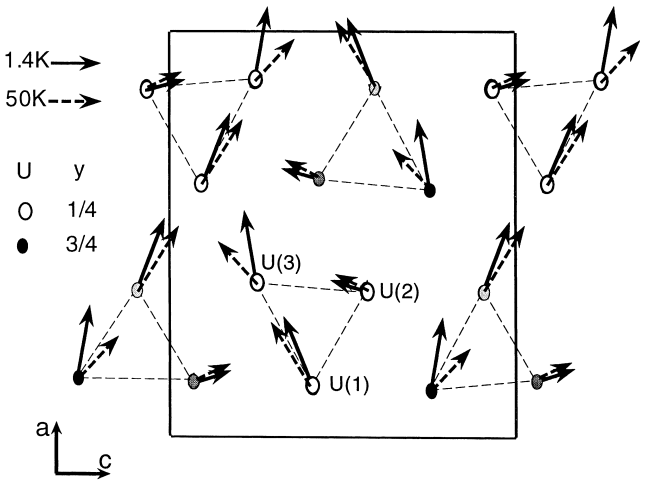

Fig. 5. 'Superposition' of the magnetic structures of U_3Te_5 at 1.4 and 50 K in the (a,c) projection plane.

Table 3
Magnetic moments (M_x, 0, M_z) for U_1, U_2, U_3 in U_3Te_5 at 1.4 K, 37 K, 50 K and 69 K (Cartesian coordinates)

T (K)	M_x U_1 (μ_B)	M_z U_1 (μ_B)	M_x U_2 (μ_B)	M_z U_2 (μ_B)	M_x U_3 (μ_B)	M_z U_3 (μ_B)
1.4	+1.74(11)	±0.63(24)	+0.29(12)	±0.87(22)	+1.80(9)	±0.24(23)
37	+1.88(10)	±0.69(18)	+0.18(11)	±1.16(17)	+1.50(10)	±0.01(18)
50	+1.57(18)	±0.97(20)	+0.39(14)	±0.81(22)	+1.07(16)	±0.88(16)
69	1.37(17)	±1.08(17)	+0.13(15)	±0.90(20)	+1.07(14)	±0.98(14)

mainly located on U_3 site, occurs between 37 and 50 K, in agreement with the thermal variations of magnetic Bragg peaks observed in Fig. 4, and with the discontinuity in the magnetization's thermal variation (Fig. 1). This 'transition' is then only a spin reorientation.

As a matter of comparison between neutron diffraction and magnetic measurements results, let us calculate the mean value of the ferromagnetic moment per uranium atom: from Table 3, we get 1.3(1) μ_B/U at $T=1.4$ K, in reasonable agreement with 0.8 μ_B as deduced from the macroscopic magnetization measurement on powder with a random orientation of the grains.

3.2. U_2Te_3 crystal and magnetic structures

The previous X-ray structure determination is confirmed by the neutron powder diffraction data, with no structural transition in the temperature range 1.4–300 K: see Table 4 for the main values of the refined parameters.

Fig. 6 shows the neutron powder diffraction diagram for U_2Te_3 at $T=1.4$ K; as for U_3Te_5 all magnetic Bragg peaks can be indexed within the chemical unit cell, i.e. with a propagation vector $k=(0\ 0\ 0)$. Fig. 7 shows the thermal variation of the integrated intensity of some characteristic peaks. From these thermal variations, we observe three characteristic magnetic 'transition' temperatures: $T=110\pm5$ K, $T=95\pm5$ K and $T=50\pm10$ K.

The best agreement with the low temperature neutron powder diffraction diagrams is obtained, whatever the temperature below 95 K, for the non-collinear antiferromagnetic G_x A_z type-structure (Bertaut's representation analysis of magnetic structures, see above). Table 5 lists the results of these magnetic refinements, in terms of magnetic moments values for U_1, U_2 and reliability factors. Below $T_C=95$ K, the magnetic order of the two

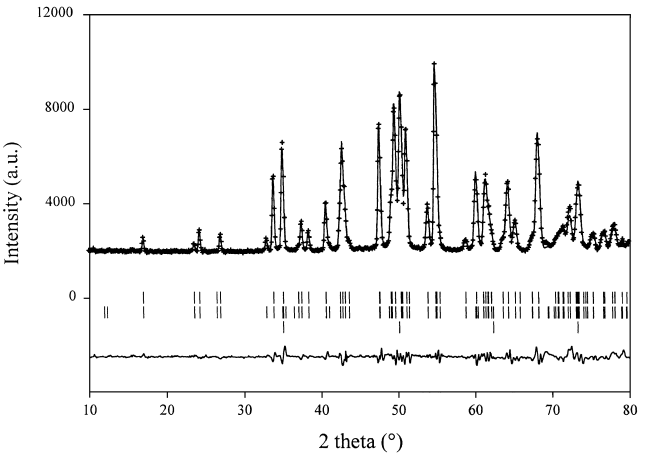

Fig. 6. U_2Te_3, $T=1.4$ K: experimental (dots) and calculated (solid line) neutron powder diffraction diagram; difference curve below. The ticks, respectively indicate the 2θ values for nuclear and magnetic Bragg peaks of U_3Te_5 (upper and middle row) and nuclear Bragg peaks of CsCl (lower row).

Table 4
U_2Te_3: refined cell parameters and atomic coordinates for U atoms, from neutron powder diffraction data at $T=155$ and 1.4 K; reliability factors R_B And R_M are calculated for nuclear and magnetic contributions, respectively

		$T=155$ K	$T=1.4$ K
a (Å)		12.179(1)	12.1623(7)
b (Å)		4.3703(4)	4.3565(2)
c (Å)		11.826(1)	11.8109(7)
U_1	x	0.0168(4)	0.0155(4)
	z	0.3134(5)	0.3139(5)
U_2	x	0.1981(4)	0.1989(5)
	z	0.0002(5)	0.0003(6)
R_B [a]		2.86	3.51
R_M [a]			8.09
No. of refined parameters		18	22

[a] Reliability factors are defined in Ref. [4].

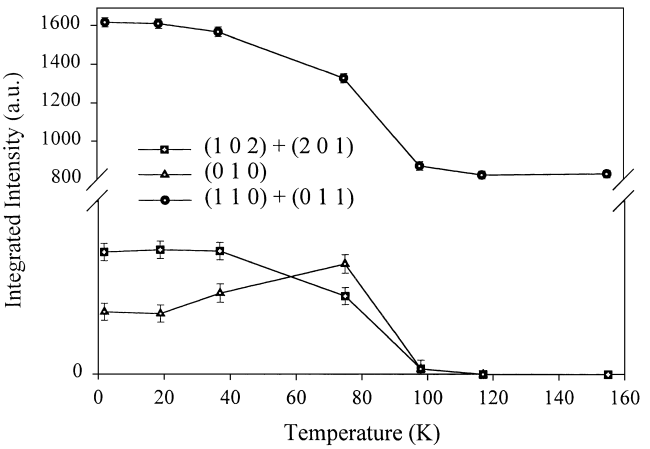

Fig. 7. U_2Te_3: thermal variation of the integrated intensity of some characteristic peaks.

Table 5
U_2Te_3: refined magnetic moments for U_1 and U_2, from neutron powder diffraction data at T ranging from 1.4 to 75 K; reliability factors R_B and R_M are calculated for nuclear and magnetic contributions, respectively

T (K)	R_N (%)	R_M (%)	M U_1 (μ_B)	M U_2 (μ_B)
1.4	3.51	8.09	2.28(5)	2.16(5)
19	3.37	8.44	2.20(5)	2.13(5)
37	2.97	8.86	2.33(5)	2.24(5)
75	3.82	11.4	1.89(6)	2.07(6)

independent uranium atoms (U_1, U_2) is non-collinear, with for each of the uranium sublattices, two antiferromagnetic components in the a–c plane. Along the a axis and the c axis, the magnetic moment components are antiferromagnetically coupled to each other but with different + and − spin sequences (see Fig. 8 at $T=1.4$ K).

As T increases from 1.4 to 95 K we observe a decreasing of the U_1 and U_2 magnetic moment amplitude and a slight rotation of essentially the U_2 magnetic moment towards the c axis occurring between 37 and 75 K (see Table 6), in agreement with the thermal variation of magnetic Bragg peaks observed in Fig. 7 ('transition' temperature: 50±10 K) and with the discontinuity in the magnetization's thermal variation (Fig. 2).

In view of the ferromagnetic behaviour revealed by the magnetization measurements we have tested an additional F_y ferromagnetic mode (allowed by Bertaut's representation group theory) in the refinement but this did not improve significantly the fit: the weakness (0.08 μ_B) of this ferromagnetic component is beyond the sensitivity of the neutron powder diffraction technique.

Above 95 K and up to 110 K the neutron diagrams are characterized by two new features: very weak additional magnetic reflections, not simply indexed, and magnetic diffuse scattering. This may be ascribed to some precursor effects in which short range spin correlations on a few unit cells are superposed to a possibly modulated (incommensurate?) magnetic structure. The magnetization anomaly observed at 105 K is probably linked to this complex intermediate magnetic structure present in the neutron diagrams from 95 to 110 K.

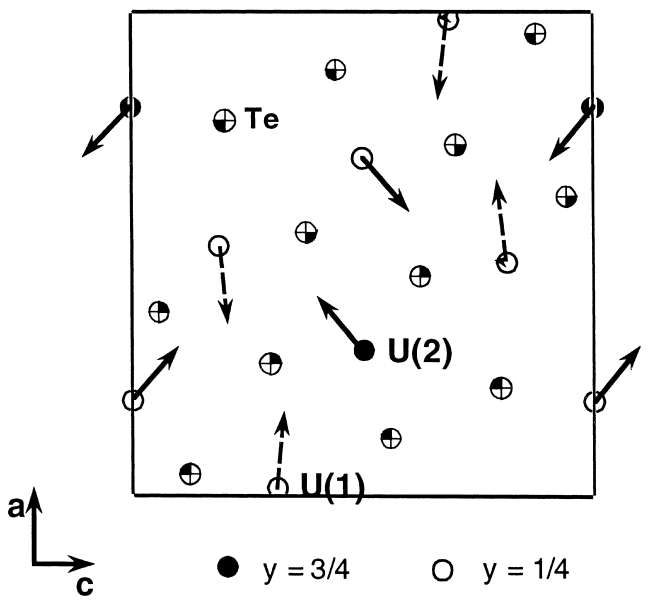

Fig. 8. Magnetic structure of U_2Te_3 at 1.4 K (projection on the a–c plane).

Table 6
Magnetic moments (M_x, 0, M_z) for U_1, U_2 in U_2Te_3 at 1.4 and 75 K (Cartesian coordinates)

T (K)	M_x U_1 (μ_B)	M_z U_1 (μ_B)	M_x U_2 (μ_B)	M_z U_2 (μ_B)
1.4	±2.43(4)	±0.13(8)	±1.71(5)	±1.54(5)
75	±1.32(3)	±0.24(5)	±0.89(4)	±1.09(4)

4. Conclusion

The two binary uranium tellurides U_2Te_3 and U_3Te_5 exhibit noncollinear magnetic structures resulting from the competition between exchange interactions and crystal field effects. Both compounds have close ordering temperatures (110 and 120 K, respectively) and show spin reorientations around 45 K. The determination of the magnetic structure of U_3Te_5 at 1.4 K revealed that the magnetic moment of the uranium located on the U_2 crystallographic site, (M $U_2=0.98(20)$ μB) is significantly lower than the magnetic moments of the uranium located on U_1 and U_3 positions, (M $U_1=1.84(10)$ μ_B, M $U_3=1.83(10)$ μ_B). The bond valence calculations [6] previously applied [1] suggest intermediate valence for all the uranium cations, with U_2 probably in a higher valence state (close to U^{4+}) than U_1 and U_3 (close to U^{3+}). For U_2Te_3, the magnetic moments at 1.4 K of the two independent uranium atoms per unit-cell U_1 and U_2 have larger values (M $U_1=2.28(5)$ μ_B and M $U_2=2.16(5)$ μ_B) than those in U_3Te_5. Considering the weak electrical conductivity [7] and to balance the charges, the uranium atoms are expected to be in trivalent oxidation state in U_2Te_3. These observations may thus illustrate a trend of an increase of the value of the localized magnetic moment from U^{4+} ($5f^2$) to U^{3+} ($5f^3$) in tellurides. In all cases, the ordered moments are much lower than the theoretical free ion values (gJ) of 3.27 and 3.20 μB for U^{3+} and U^{4+}, respectively.

References

[1] O. Tougait, M. Potel, H. Noël, J. Solid State Chem. 139 (1998) 356.

[2] O. Tougait, J.C. Levet, M. Potel, H. Noël, Eur. J. Solid State Inorg. Chem. 35 (1998) 67.
[3] W. Suski, Bull. Acad. Pol. Sci. 24 (1976) 75.
[4] J. Rodriguez-Caravajal, in: Abst. Satellite Meeting Powder Diffraction, 15th Congress of the I.U.C., Toulouse, France, 1990.
[5] E.F. Bertaut, Acta Cryst. A24 (1968) 217.
[6] N.E. Breze, M. O'Keeffe, Acta Crystallogr. B47 (1991) 192.
[7] A. Blaise, B. Janus, W. Suski, Solid State Commun. 37 (1981) 417.